27. Tanner A, Bochner F, Caffin J, Halliday J, Powell L. Dose-dependent prednisolone kinetics. Clin Pharmacol Ther **1979**; 25:571–8.
28. Toulza F, Heaps A, Tanaka Y, Taylor GP, Bangham CR. High frequency of CD4+FoxP3+ cells in HTLV-1 infection: inverse correlation with HTLV-1-specific CTL response. Blood **2008**; 111:5047–53.
29. Shimizu Y, Takamori A, Utsunomiya A, et al. Impaired Tax-specific T-cell responses with insufficient control of HTLV-1 in a subgroup of individuals at asymptomatic and smoldering stages. Cancer Sci **2009**; 100:481–9.
30. Ando H, Sato T, Tomaru U, et al. Positive feedback loop via astrocytes causes chronic inflammation in virus-associated myelopathy. Brain **2013**; 136:2876–87.
31. Machigashira K, Ijichi S, Nagai M, Yamano Y, Hall WW, Osame M. In vitro virus propagation and high cellular responsiveness to the infected cells in patients with HTLV-I-associated myelopathy (HAM/TSP). J Neurol Sci **1997**; 149:141–5.
32. Sakai JA, Nagai M, Brennan MB, Mora CA, Jacobson S. In vitro spontaneous lymphoproliferation in patients with human T-cell lymphotropic virus type I-associated neurologic disease: predominant expansion of CD8+ T cells. Blood **2001**; 98:1506–11.
33. Nagai M, Usuku K, Matsumoto W, et al. Analysis of HTLV-I proviral load in 202 HAM/TSP patients and 243 asymptomatic HTLV-I carriers: high proviral load strongly predisposes to HAM/TSP. J Neurovirol **1998**; 4:586–93.
34. Iwanaga M, Watanabe T, Utsunomiya A, et al. Human T-cell leukemia virus type I (HTLV-1) proviral load and disease progression in asymptomatic HTLV-1 carriers: a nationwide prospective study in Japan. Blood **2010**; 116:1211–9.
35. Geginat J, Lanzavecchia A, Sallusto F. Proliferation and differentiation potential of human CD8+ memory T-cell subsets in response to antigen or homeostatic cytokines. Blood **2003**; 101:4260–6.
36. Kondo T, Takiguchi M. Human memory CCR4+CD8+ T cell subset has the ability to produce multiple cytokines. Int Immunol **2009**; 21: 523–32.
37. Baek HJ, Zhang L, Jarvis LB, Gaston JS. Increased IL-4+ CD8+ T cells in peripheral blood and autoreactive CD8+ T cell lines of patients with inflammatory arthritis. Rheumatology (Oxford) **2008**; 47:795–803.
38. Nagai M, Kubota R, Greten TF, Schneck JP, Leist TP, Jacobson S. Increased activated human T cell lymphotropic virus Type I (HTLV-I) Tax11–19-specific memory and effector CD8+ cells in patients with HTLV-I-associated myelopathy/tropical spastic paraparesis: correlation with HTLV-I provirus load. J Infect Dis **2001**; 183:197–205.
39. Yasunaga J, Sakai T, Nosaka K, et al. Impaired production of naive T lymphocytes in human T-cell leukemia virus type I-infected individuals: its implications in the immunodeficient state. Blood **2001**; 97:3177–83.
40. Joshi NS, Cui W, Chandele A, et al. Inflammation directs memory precursor and short-lived effector CD8+ T cell fates via the graded expression of T-bet transcription factor. Immunity **2007**; 27:281–95.
41. Kannagi M, Hasegawa A, Kinpara S, Shimizu Y, Takamori A, Utsunomiya A. Double control systems for human T-cell leukemia virus type 1 by innate and acquired immunity. Cancer Sci **2011**; 102:670–6.
42. Hanon E, Hall S, Taylor GP, et al. Abundant tax protein expression in CD4+ T cells infected with human T-cell lymphotropic virus type I (HTLV-I) is prevented by cytotoxic T lymphocytes. Blood **2000**; 95: 1386–92.
43. Vine AM, Heaps AG, Kaftantzi L, et al. The role of CTLs in persistent viral infection: cytolytic gene expression in CD8+ lymphocytes distinguishes between individuals with a high or low proviral load of human T cell lymphotropic virus type 1. J Immunol **2004**; 173:5121–9.
44. Hanon E, Stinchcombe JC, Saito M, et al. Fratricide among CD8+ T lymphocytes naturally infected with human T cell lymphotropic virus type I. Immunity **2000**; 13:657–64.
45. Sugiyama D, Nishikawa H, Maeda Y, et al. Anti-CCR4 mAb selectively depletes effector-type FoxP3+CD4+ regulatory T cells, evoking antitumor immune responses in humans. Proc Natl Acad Sci U S A **2013**; 110:17945–50.
46. Ishida T, Ueda R. Immunopathogenesis of lymphoma: focus on CCR4. Cancer Sci **2011**; 102:44–50.

ANNALS of Clinical and Translational Neurology
Open Access
AMERICAN NEUROLOGICAL ASSOCIATION

RESEARCH ARTICLE

A plasma diagnostic model of human T-cell leukemia virus-1 associated myelopathy

Makoto Ishihara[1], Natsumi Araya[2], Tomoo Sato[2], Naomi Saichi[1], Risa Fujii[1], Yoshihisa Yamano[2] & Koji Ueda[1]

[1]Division of Biosciences, Functional Proteomics Center, Graduate School of Frontier Sciences, The University of Tokyo, Tokyo, Japan
[2]Department of Rare Diseases Research, Institute of Medical Science, St. Marianna University School of Medicine, Kawasaki, Japan

Correspondence
Koji Ueda, Division of Biosciences, Functional Proteomics Center, Graduate School of Frontier Sciences, The University of Tokyo, CREST hall 1F, Institute of Medical Science, 4-6-1 Shirokanedai, Minato-ku, Tokyo, Japan, 108-8639. Tel: +81-3-6409-2062; Fax: +81-3-6409-2063; E-mail: k-ueda@ims.u-tokyo.ac.jp

Funding Information
This work was supported by grant-in-aid for Research Project on Overcoming Intractable Diseases from the Ministry of Health Labour and Welfare Japan and grant-in-aid for Young Scientists (B) (23701090) from the Ministry of Education, Culture, Sports, Science & Technology Japan.

Received: 19 November 2014; Accepted: 9 December 2014

***Annals of Clinical and Translational Neurology* 2015; 2(3): 231–240**

doi: 10.1002/acn3.169

Abstract

Objective: Human T-cell leukemia virus-1 (HTLV-1) associated myelopathy/tropic spastic paraparesis (HAM/TSP) is induced by chronic inflammation in spinal cord due to HTLV-1 infection. Cerebrospinal fluid (CSF) neopterin or proviral load are clinically measured as disease grading biomarkers, however, they are not exactly specific to HAM/TSP. Therefore, we aimed to identify HAM/TSP-specific biomarker molecules and establish a novel less-invasive plasma diagnostic model for HAM/TSP. **Methods**: Proteome-wide quantitative profiling of CSFs from six asymptomatic HTLV-1 carriers (AC) and 51 HAM/TSP patients was performed. Fourteen severity grade biomarker proteins were further examined plasma enzyme-linked immunosorbent assay (ELISA) assays (n = 71). Finally, we constructed three-factor logistic regression model and evaluated the diagnostic power using 105 plasma samples. **Results**: Quantitative analysis for 1871 nonredundant CSF proteins identified from 57 individuals defined 14 CSF proteins showing significant correlation with Osame's motor disability score (OMDS). Subsequent ELISA experiments using 71 plasma specimens confirmed secreted protein acidic and rich in cysteine (SPARC) and vascular cell adhesion molecule-1 (VCAM-1) demonstrated the same correlations in plasma (R = −0.373 and R = 0.431, respectively). In this training set, we constructed a HAM/TSP diagnostic model using SPARC, VCAM1, and viral load. Sensitivity and specificity to diagnose HAM/TSP patients from AC (AC vs. OMDS 1–11) were 85.3% and 81.1%, respectively. Importantly, this model could be also useful for determination of therapeutic intervention point (OMDS 1–3 + AC vs. OMDS 4–11), exhibiting 80.0% sensitivity and 82.9% specificity. **Interpretation**: We propose a novel less-invasive diagnostic model for early detection and clinical stratification of HAM/TSP.

Introduction

The RNA retrovirus human T-cell leukemia virus-1 (HTLV-1) is endemic in Japan, Caribbean basin, Iran, Africa, South America, and the Melanesian islands.[1] Number of infected individuals is currently estimated at around 30 million worldwide,[2] in which 5% of virus carriers develop HTLV-1 associated myelopathy/tropic spastic paraparesis (HAM/TSP) or adult T-cell leukemia (ATL) after asymptomatic phase of typically over 30 years. Inflammation of spinal cord is a principal symptom of HAM/TSP patients, causing progressive scelotyrbe, gait impairment, or urination disorder.[3] However, no curative therapy for HAM/TSP has been developed except for anti-inflammatory treatments by INF-α or steroids,[4] whereas excessive or long-term use of these drugs can increase the risk of adverse events.[5,6] Hence, the treatment regimens should be carefully managed based on a thorough assessment of disease stage and activity. As for the severity grading of HAM/TSP, Osame's motor disability score (OMDS) is widely used to define disease stages and estimate the rate of disease progression.[7] Although this scale is helpful to evaluate consequential impairment of motor functions, development of molecular-based

diagnostics has been a major challenge for early detection and adequate therapeutic intervention of HAM/TSP.

To identify HAM/TSP-specific biomarkers, a variety of genomic or proteomic analyses were performed for infected T cells and plasma samples,[8-10] however, comprehensive investigation for cerebrospinal fluid (CSF) has not been launched in spite of the most fundamental site of HAM/TSP lesion. Therefore, we intended to acquire the first proteome-wide view of CSFs reflecting HAM/TSP-associated alteration of spinal cord microenvironment. Following the statistical identification of severity grade biomarkers from CSFs, we attempted to construct a HAM/TSP diagnostic model using less-invasive plasma specimens.

Subjects and Methods

Participants

CSF specimens (from 51 HAM/TSP patients and six asymptomatic carriers [ACs]) and plasma specimens (from 50 HAM/TSP patients and 55 ACs) were collected in St. Marianna University School of Medicine and kept frozen at −80°C until just before use. The research procedure was explained and written informed consent was obtained from all the patients. This study was approved by the Ethical Committee of the University of Tokyo (approval code 14-1) and the Ethical Committee of St. Marianna University School of Medicine.

LC/MS/MS analysis

The 20 μL each of CSFs was lyophilized and dissolved in 8 mol/L Urea (GE Healthcare, Buckinghamshire, UK) in 50 mmol/L ammonium bicarbonate (Sigma-Aldrich, St. Louis, MO). After reduction with 5 mmol/L tris(2-carboxyethyl)phosphine (Sigma-Aldrich) at 37°C for 30 min, proteins were alkylated with 25 mmol/L Iodoacetamide (Sigma-Aldrich) at ambient temperature for 45 min. Following fourfold dilution with 50 mmol/L ammonium bicarbonate, proteins were digested with immobilized trypsin (Thermo Scientific, Bremen, Germany) at 37°C for 6 h. Digested samples were then desalted by Oasis HLB μElution plate (Waters, Milford, MA) and analyzed by liquid chromatography - tandem mass spectrometry (LC/MS/MS). The peptides were separated on Ultimate 3000 RSLC nano-HPLC system (Thermo Scientific) equipped with 0.075 × 150 mm C_{18} tip-column (Nikkyo Technos, Tokyo, Japan) using two-step linear gradient comprising 2–35% acetonitrile for 95 min and 35–95% acetonitrile for 15 min in 0.1% formic acid at the flow rate of 250 nL/min. The eluates were analyzed with LTQ Orbitrap Velos mass spectrometer (Thermo Scientific). Spectra were collected using full MS scan mode over the mass-to-charge (*m/z*) range 400–1600. MS/MS was performed on the top 20 ions in each MS scan using the data-dependent acquisition mode with dynamic exclusion enabled.

2D-LC/MS/MS analysis

CSF tryptic digests were resolved in 10 mmol/L ammonium formate (Sigma-Aldrich) in 25% acetonitrile and fractionated with 0.2 × 250 mm strong cation exchange monolith column (GL Science, Tokyo, Japan). The samples were eluted with the gradient from 10 mmol/L to 1 mol/L of ammonium formate in curve = 3 mode within 70 min using Prominence HPLC system (Shimadzu Corporation, Kyoto, Japan). The eluate was separated into 11 fractions and analyzed by LC/MS/MS.

Protein/peptide identification

MS/MS spectra were searched against SwissProt database version 2012_06 (20,232 human protein sequences) using SEQUEST algorithm on ProteomeDiscoverer 1.3 software (Thermo Scientific). Proteins satisfying the false discovery rate (FDR) <1% by Peptide Validator FDR estimation algorithm on ProteomeDiscoverer was accepted. Gene ontology (GO) term analysis was performed using DAVID Bioinformatics Resources 6.7 (http://david.abcc.ncifcrf.gov/).

Label-free quantification analysis

The LC/MS/MS data from 57 CSF samples were imported on the Expressionist server (Genedata AG, Basel, Swiss) and processed along the workflow shown in Figure S1. The four-step Chromatogram Chemical Noise Subtraction was performed, composed of (1) RT structure removal = true, minimum RT length = 2 scans, (2) *m/z* structure removal = true, minimum *m/z* length = 6 scans, (3) RT window = 501 scans, quantile subtraction = 90%, and (4) RT structural removal = true, minimum RT length = 2 scans. Data points with intensity <500 were clipped to zero. Again, Chromatogram Chemical Noise Subtraction was performed using chromatogram smoothing = true, RT windows = 5 scans, and estimator = Moving average. After applying Chromatogram Grid with a distance of scan counts = 10, RT variety among 57 samples was normalized by Chromatogram RT Alignment: *m/z* windows = 11 points, RT windows = 11 scans, gap penalty = 1, RT search interval = 2 min, alignment scheme = pairwise alignment based tree. Peaks were detected by Chromatogram Summed Peak Detection: summation window = 20 scans, overlap = 10, minimum peak size = 6 scans, maximum merge distance = 1 point,

peak RT splitting = true, intensity profiling = maximum, gap/peak ratio = 5%, refinement threshold = 80, consistency threshold = 1. The detected peaks were grouped in isotopic clusters using Chromatogram Isotopic Peak Clustering: minimum charge = 1, maximum charge = 10, maximum missing peaks = 0, first allowed gap position = 10, RT window = 0.02 min, *m/z* tolerance = 5 ppm, isotope shape tolerance = 10, minimum cluster size ration = 0.5.

Cytometric bead array

Concentration of C-X-C motif chemokine 10 (CXCL10) in CSF was determined by cytometric bead array (CBA) (BD Biosciences, San Jose, CA) according to the manufacturer's instructions.

Enzyme-linked immunosorbent assay

Concentrations of secreted protein acidic and rich in cysteine (SPARC) (R&D Systems, Minneapolis, MN) and vascular cell adhesion molecule-1 (VCAM1) (Abcam, Cambridge, MA) in 105 plasma samples were measured with commercial enzyme-linked immunosorbent assay (ELISA) kit following the manufacturer's instructions. A multivariate logistic regression was applied to construct a new diagnostic model for HAM/TSP utilizing three factors, SPARC, VCAM1, and viral load, as described previously.[11]

Result

Quantitative proteome profiling of CSFs from HAM/TSP patients

CSFs from 6 ACs and 51 HAM/TSP patients (Table 1) were processed according to the schematic workflow of this study (Fig. 1). Nonredundant 68,077 peptides from 57 individuals were detected and quantified on the Expressionist proteome server system, meanwhile 14,451

Table 1. Clinical characteristics of the CSF specimens.

Group	*N*	Age (±SD)	Gender (M/F)
AC	6	55.7 (±15.8)	4/2
HAM1_3	7	57.9 (±14.2)	3/4
HAM4_6	35	59.3 (±11.0)	11/24
HAM7_11	9	61.6 (±8.0)	1/8
Total	57	59.1 (±11.7)	19/38

CSF, cerebrospinal fluid; AC, asymptomatic carriers; HAM1_3, HAM/TSP patients whose Osame's motor disability score from 1 to 3; HAM4_6, HAM/TSP patients whose Osame's motor disability score from 4 to 6; HAM7_11, HAM/TSP patients whose Osame's motor disability score from 7 to 11.

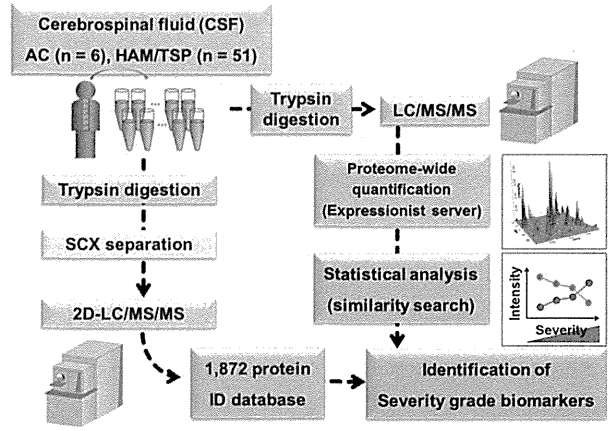

Figure 1. Schematic overview of severity grade marker screening. Cerebrospinal fluids (CSFs) from six asymptomatic carriers (ACs) and 51 HAM/TSP patients were analyzed by LC/MS/MS. Candidate peptides whose intensities had correlation with severity grades were isolated according to Pearson product-moment correlation coefficient. Candidate peptides were identified using Protein/Peptide identification database established by 2D-LC/MS/MS. HAM/TSP, human T-cell leukemia virus-1 associated myelopathy/tropic spastic paraparesis.

CSF peptides (1871 proteins) were identified by parallel 2D-LC/MS/MS analysis. To evaluate quantitative reliability of our LC/MS-based proteome profiling, observed relative concentrations of CXCL10 (Interferon gamma Inducible protein 10, CXCL10) were compared to clinical data which were measured by CBA (Fig. 2A). The result showed strong correlation (R^2 = 0.911) between two measurements, indicating that our LC/MS-based quantification results were highly credible even in the low concentration range (1–20 ng/mL).

Next, to interpret proteome-wide alterations in CSF environment of HAM/TSP patients, 1345 or 1750 proteins identified from AC or HAM/TSP patients group, respectively (Fig. 2B), were classified according to cellular component (CC, Fig. 2C and D) or biological process (BP, Fig. 2E and F) using DAVID Functional Annotation Tool. The CC analysis revealed that proteins expressed in cell projection and plasma membrane were enriched in CSF of HAM/TSP patients, in addition to specific enrichment of viral proteins. This may reflect increased invasive activity of HTLV-1-infected cells into spinal cord, which is often observed in HAM/TSP patients. Further BP analysis indicated that proteins involved in cell adhesion, cell motion, cell migration, cytoskeleton, and cell structure disassembly were highly enriched in CSF of HAM/TSP patients. These features also denoted proteome-wide environmental change in spinal cord, inducing active migration and/or invasion of lymphocytes. Proteins related to cell death and cell growth might associate with spinal inflammation in HAM/TSP patients.

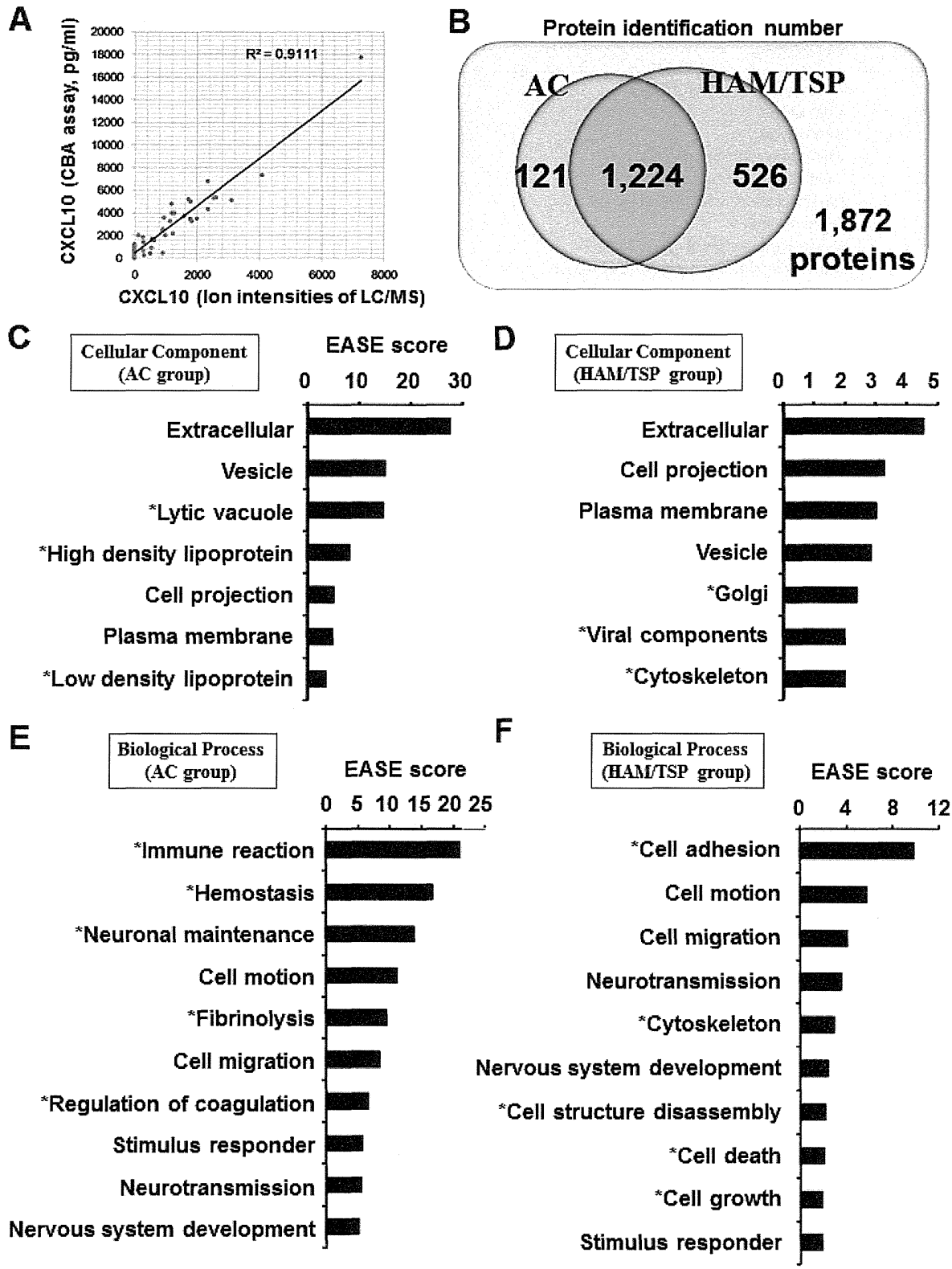

Table 2. List of 16 severity grade markers for HAM/TSP.

UniProt accession	Protein name	Amino acid numbers of identified peptide	Pearson's correlation coefficient (*R*)	*P*-value
Q9NZK5	Adenosine deaminase CECR1	247–258	0.478	5.15E-04
Q12860	Contactin-1	634–647	−0.425	9.94E-04
Q14118	Dystroglycan	222–232	−0.463	2.89E-04
Q8N2S1	Latent-transforming growth factor beta-binding protein 4	310–323	−0.463	2.90E-04
Q9Y5Y7	Lymphatic vessel endothelial hyaluronic acid receptor 1	8–18	−0.499	9.15E-05
Q16653	Myelin-oligodendrocyte glycoprotein	14–25	−0.444	5.40E-04
Q9UJJ9	N-acetylglucosamine-1-phosphotransferase subunit gamma	47–56	−0.442	5.72E-04
P13591	Neural cell adhesion molecule 1	586–597	−0.459	3.31E-04
P36955	Pigment epithelium-derived factor	133–141	−0.454	3.83E-04
Q9UHG2	ProSAAS	14–24	−0.444	5.42E-04
P09486	Secreted protein acidic and rich in cysteine	124–133	−0.523	3.01E-05
P09486	Secreted protein acidic and rich in cysteine	156–164	−0.477	1.75E-04
P09486	Secreted protein acidic and rich in cysteine	252–262	−0.457	3.55E-04
Q92563	Testican-2	139–148	−0.424	1.03E-03
Q06418	Tyrosine-protein kinase receptor TYRO3	279–290	−0.438	1.04E-03
P19320	Vascular cell adhesion protein 1	581–590	0.430	9.35E-04

HAM/TSP, human T-cell leukemia virus-1 associated myelopathy/tropic spastic paraparesis.

Statistical analysis for screening severity grade marker candidates

To extract biomarker proteins showing stoichiometric increase/decrease in accordance with progression of HAM/TSP, numerical classes (0, 1, 2, and 3) were given to four clinically relevant severity groups (AC, HAM/TSP OMDS 1–3, 4–6, and 7–11, respectively) (see Table S1). Then quantitative correlation between severity classes and 68,077 peptide intensities was ranked with Pearson's correlation analysis. Peptides with the lowest 100 *P*-values (Table S2) were next subjected to protein identification analysis by 2D-LC/MS/MS, resulting in successful identification of 14 proteins derived from 16 peptides (Table 2). In addition to Pearson's correlation coefficients and *P*-values in Table 2, LC/MS-based quantitative profiles of 16 peptides were illustrated with box plots (Fig. 3). Compared to a traditional severity grade marker neopterin ($R = 0.4105$, $P = 1.12E\text{-}03$), any of identified proteins showed better potential to be utilized as CSF disease state biomarkers.

SPARC and VCAM-1 as HAM/TSP severity grade markers in plasma

To further narrow down the biomarker candidates and establish plasma-based less-invasive diagnostics, we examined plasma levels of the 14 proteins by ELISA assays measuring 71 training cases (Table 3). The results revealed that a couple of proteins, SPARC and VCAM1, showed the same correlation in plasma with CSF levels ($|R| > 0.4$ and $P < 0.05$) (Fig. 4A and B). Therefore, we attempted construction of the combination biomarker diagnostics using newly identified two proteins and HTLV-1 viral load, all of which are measurable from small volume of blood samples. In order to halt the progression of HAM/TSP and maintain better quality of life for patients, both early diagnosis of HAM/TSP onset and therapeutic intervention at appropriate time point are essential. On the basis of these clinical requirements, we made two logistic regression models which maximized area under the curve (AUC) of ROC curves comparing ACs with HAM/TSP patients (onset predictor; (1)) or

Figure 2. Summary of CSF proteome. (A) Evaluation of LC/MS-based quantification analysis. The relative concentrations of CXCL10 cytokine calculated by mass spectrometric analysis were compared to independent measurements by cytometric bead array (CBA). (B) Venn diagram of identified proteins in 57 CSF analyses. The Gene Ontology (GO) analysis using DAVID Bioinformatics Resources displayed enriched cellular components of CSF proteins in ACs (C) or HAM/TSP patients (D). The enriched biological functions of CSF proteins in ACs (E) or HAM/TSP patients (F) were also shown. Expression Analysis Systematic Explorer (EASE) enrichment scores were shown. CSF, cerebrospinal fluid; CXCL10, C-X-C motif chemokine 10; ACs, asymptomatic carriers; HAM/TSP, human T-cell leukemia virus-1 associated myelopathy/tropic spastic paraparesis.

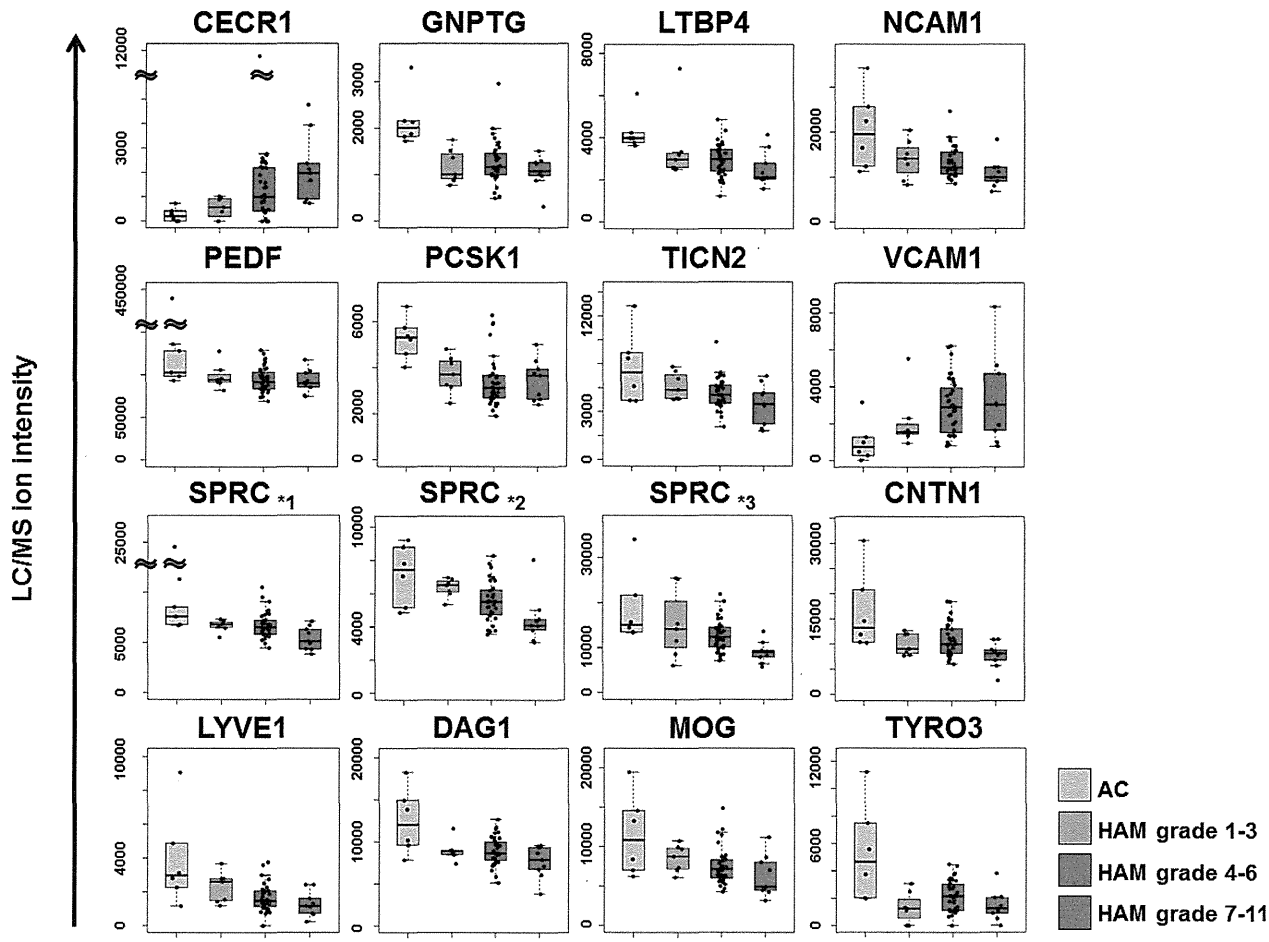

Figure 3. Panels of identified severity grade marker candidates for HAM/TSP. Box plots of 16 peptides derived from 14 candidate proteins are displayed. The Y axis stands for the LC/MS ion intensities. *1, *2, and *3 correspond to distinct SPARC-derived peptides. Amino acid numbers of peptides are as follows: *1; 124–133, *2; 156–164, *3; 252–262. HAM/TSP, human T-cell leukemia virus-1 associated myelopathy/tropic spastic paraparesis; SPARC, secreted protein acidic and rich in cysteine.

Table 3. Clinical characteristics of the plasma specimens.

Group	*N*	Age (±SD)	Gender (M/F)
Training cases			
AC	37	51.5 (±13.2)	13/24
HAM1_3	4	55.0 (±4.7)	3/1
HAM4_6	20	60.5 (±10.8)	4/16
HAM7_11	10	62.0 (±8.2)	2/8
Test cases			
AC	18	54.2 (±12.3)	4/14
HAM1_3	2	59.5 (±12.0)	0/2
HAM4_6	9	56.8 (±14.9)	4/5
HAM7_11	5	71.2 (±2.9)	0/5

AC, asymptomatic carriers; HAM1_3, HAM/TSP patients whose Osame's motor disability score range from 1 to 3; HAM4_6, HAM/TSP patients whose Osame's motor disability score range from 4 to 6; HAM7_11, HAM/TSP patients whose Osame's motor disability score range from 7 to 11.

ACs + HAM/TSP OMDS 1–3 with HAM/TSP OMDS 4–11 (therapeutic intervention predictor; (2)).

$$\log\left(\frac{P(x)}{1-P(x)}\right) = -11.19 - 0.01980\ (\text{SPARC}) + 0.009322\ (\text{VCAM1}) + 0.1142\ (\text{Viral Load}) \quad (1)$$

$$\log\left(\frac{P(x)}{1-P(x)}\right) = -11.73 - 0.01808\ (\text{SPARC}) + 0.009651\ (\text{VCAM1}) + 0.09151\ (\text{Viral Load}) \quad (2)$$

Finally, we assessed our prediction models using 105 plasma samples (71 training samples with 34 independent test samples). The AUC of ROC curves in Figure 4C and D demonstrated significantly higher diagnostic powers of our three-factor models for both onset prediction

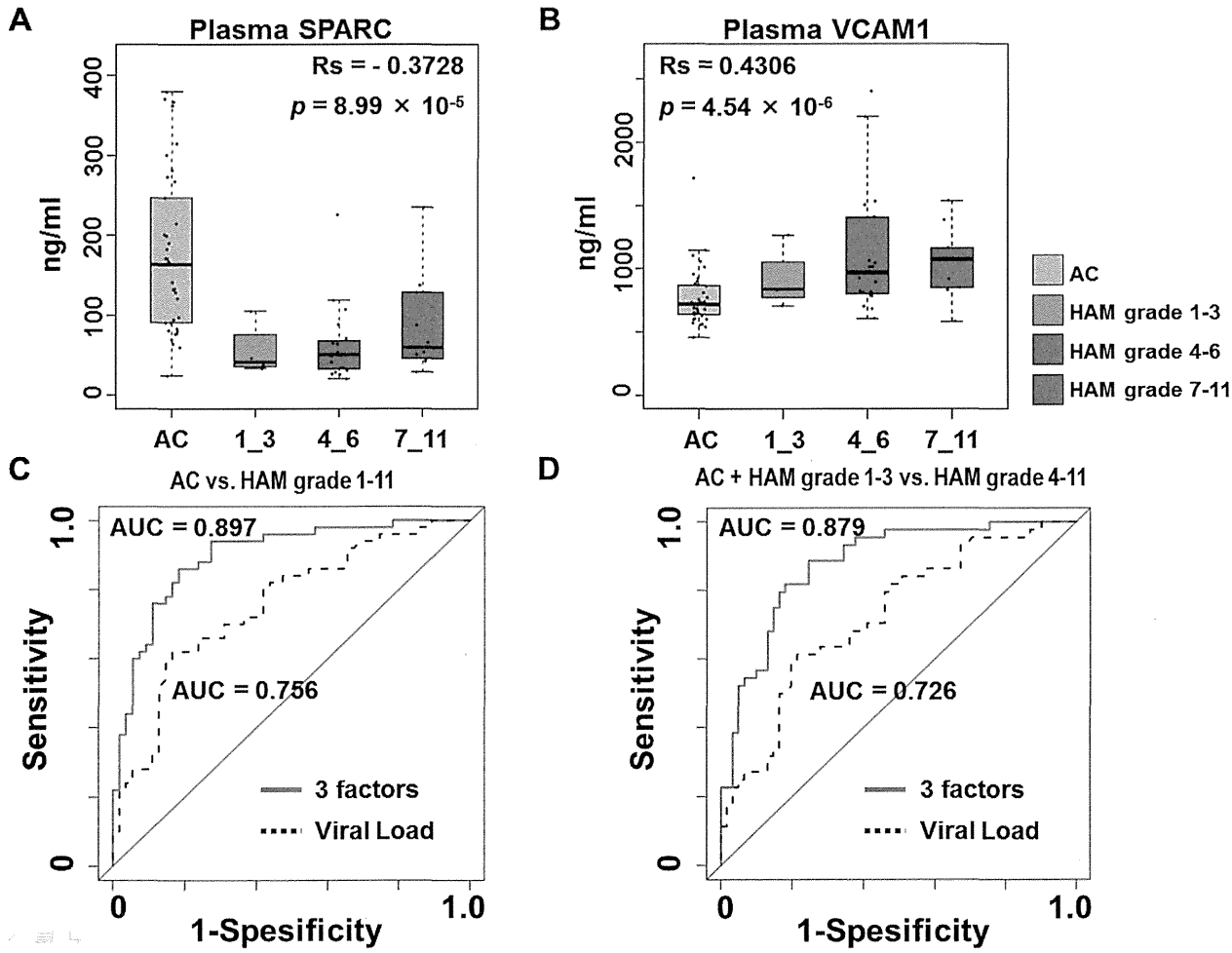

Figure 4. Construction of plasma-based diagnostic models. Plasma SPARC (A) and VCAM1 (B) were measured by ELISA assays. Pearson's correlation coefficient showed significant correlation between severity and novel markers. The three-factor logistic regression models (plasma SPARC, VCAM1, and HTLV-1 viral load) were validated with 105 samples in order for prediction of HAM/TSP onset (C) and appropriate therapeutic intervention point (D). The three-factor models showed better diagnostic performances than those of viral load only. Values of area under the curve (AUC) were shown. SPARC, secreted protein acidic and rich in cysteine; VCAM1, vascular cell adhesion molecule-1; ELISA, enzyme-linked immunosorbent assay; HTLV-1, human T-cell leukemia virus-1; HAM/TSP, human T-cell leukemia virus-1 associated myelopathy/tropic spastic paraparesis.

(AUC = 0.897) and treatment initiation point prediction (AUC = 0.879), compared to two-factor models (AUC = 0.861 and 0.856, respectively), SPARC (AUC = 0.748 and 0.736, respectively), VCAM1 (AUC = 0.768 and 0.774, respectively), and HTLV-1 viral load (AUC = 0.756 and 0.726, respectively) (Figs. S2, S3). Additionally, sensitivity and specificity of three-factor model for onset prediction were 86.0% and 81.8%, respectively, whereas those for treatment initiation point prediction were 81.8% and 82.0%, respectively (Table 4). These diagnostic yields were significantly better than those of previously reported biomarkers CSF neopterin, CSF CXCL10, and serum soluble IL-2 receptor (sIL-2R) (Table S3). Thus, our three-factor diagnostics can provide valid and noninvasive routine test for HTLV-1 carriers and HAM/TSP patients, leading to precise disease control and better clinical outcome.

Discussion

An objective and scientifically evident diagnosis should be the basis of any medical actions. However, for HAM/TSP patients, clinical decisions have been made based on subjective health complaints mainly. Although HTLV-1 viral load, serum sIL-2R, and CSF neopterin are recently accepted as severity grade indicators for HAM/TSP,[5] only

Table 4. Prediction of HAM/TSP onset and the point of therapeutic intervention.

	Onset					Point of therapeutic intervention				
Predictors	3 factors	SPARC + VCAM1	SPARC	VCAM1	Viral load	3 factors	SPARC + VCAM1	SPARC	VCAM1	Viral load
Training set (n = 71)										
Sensitivity %	85.3	82.4	76.5	79.4	55.9	80.0	73.3	76.7	60.0	53.3
Specificity %	81.1	67.6	45.9	62.2	89.2	82.9	80.5	48.8	85.4	82.9
Positive predictive value %	80.6	70.0	56.5	65.9	82.6	77.4	73.3	52.3	75.0	69.6
Negative predictive value %	85.7	80.6	68.0	76.7	68.8	85.0	80.5	74.1	74.5	70.8
AUC	0.897	0.839	0.669	0.754	0.732	0.881	0.846	0.667	0.773	0.699
Test set (n = 105)										
Sensitivity %	86.0	88.0	82.0	80.0	62.0	81.8	79.5	81.8	56.8	61.4
Specificity %	81.8	69.1	49.1	63.6	83.6	82.0	80.3	54.1	82.0	78.7
Positive predictive value %	81.1	72.1	59.4	66.7	77.5	76.6	74.5	56.3	69.4	67.5
Negative predictive value %	86.5	86.4	75.0	77.8	70.8	86.2	84.5	80.5	72.5	73.8
AUC	0.897	0.861	0.748	0.768	0.756	0.879	0.856	0.736	0.774	0.726

3 factors, logistic regression model using SPARC, VCAM1, and HTLV-1 viral load; HAM/TSP, human T-cell leukemia virus-1 associated myelopathy/tropic spastic paraparesis; AUC, area under the curve of ROC analysis.

relative increase/decrease of these biomarkers is valuable to assess efficiency of treatment. In this study, we successfully established predictive models which quantitatively define HAM/TSP disease status directly from plasma SPARC, VCAM1, and HTLV-1 viral load. This three-factor prediction model can be easily involved in routine medical examinations for ACs to monitor HAM/TSP onset because three biomarkers are measurable from a single blood collection without any invasive procedures such as CSF collection. Because progression of HAM/TSP tends to be rapid typically within a few years since the onset,[12] our prediction model for treatment initiation point will effectively prevent delay of deciding therapeutic intervention for early stage HAM/TSP patients.

Concerning physiological consideration of a new biomarker SPARC, the expression is specifically restricted within glial cells in nervous system including spinal cord.[13] In addition, encephalitis induced by *N*-methyl-D-aspartic acid (NMDA) in mice resulted in downregulation of SPARC in glial cells.[14] These facts suggested that plasma level of SPARC in HAM/TSP patients decrease along with the diminished number of glial cells caused by spinal cord degeneration and reduced expression of SPARC in glial cells which are pathological characteristics of HAM/TSP. On the other hand, CSF neopterin is known as an inflammatory small biological compound upregulated in many inflammatory neurologic diseases, such as multiple sclerosis, HIV encephalopathy, and Lyme neuroborreliosis,[15–17] indicating that neopterin cannot describe spinal cord degeneration specifically. Therefore, SPARC in plasma or CSF can be considered as more specific biomarker for HAM/TSP compared to CSF neopterin. Another new biomarker VCAM1 is expressed on the surface of endothelial cells, whose soluble form is known to be upregulated in plasma during the process of inflammation.[18] In HAM/TSP patients, VCAM1 is upregulated in inflammatory region within spinal cord.[19] Hence, diagnostic features of VCAM1 are more disease-oriented than neopterin, but VCAM1 can be measured from noninvasive blood specimens.

In conclusion, proteome-wide quantitative profiling of CSFs identified 14 severity grade biomarkers for HAM/TSP. Two of them, SPARC and VCAM1, were confirmed to be useful for plasma-based diagnosis of HAM/TSP onset and severity grades. It has long been difficult to expect a sudden onset of HAM/TSP after decades of asymptomatic phase in 0.5% of HTLV-1 carriers. Routine examination of our triple biomarkers will contribute to early diagnosis of HAM/TSP, leading to appropriate management of disease before suffering severe symptoms.

Acknowledgment

This work was supported by grant-in-aid for Research Project on Overcoming Intractable Diseases from the Ministry of Health Labour and Welfare Japan and grant-in-aid for Young Scientists (B) (23701090) from the Ministry of Education, Culture, Sports, Science & Technology Japan.

Conflict of Interest

Dr. Ueda has a patent Methods for detection and disease stage classification of HTLV-1 associated myelopathy pending. Dr. Ishihara has a patent Methods for detection and disease stage classification of HTLV-1 associated myelopathy pending. Dr. Araya has a patent Methods for detection and disease stage classification of HTLV-1 associated myelopathy pending. Dr. Saichi has a patent Methods for detection and disease stage classification of HTLV-1 associated myelopathy pending. Dr. Fujii has a patent Methods for detection and disease stage classification of HTLV-1 associated myelopathy pending. Dr. Sugano has a patent Methods for detection and disease stage classification of HTLV-1 associated myelopathy pending. Dr. Sato has a patent Methods for detection and disease stage classification of HTLV-1 associated myelopathy pending. Dr. Yamano has a patent Methods for detection and disease stage classification of HTLV-1 associated myelopathy pending.

References

1. Yamashita M, Ido E, Miura T, Hayami M. Molecular epidemiology of HTLV-I in the world. J Acquir Immune Defic Syndr Hum Retrovirol 1996;13(suppl 1):S124–S131.
2. Asquith B, Zhang Y, Mosley AJ, et al. In vivo T lymphocyte dynamics in humans and the impact of human T-lymphotropic virus 1 infection. Proc Natl Acad Sci USA 2007;104:8035–8040.
3. Enose-Akahata Y, Abrams A, Johnson KR, et al. Quantitative differences in HTLV-I antibody responses: classification and relative risk assessment for asymptomatic carriers and ATL and HAM/TSP patients from Jamaica. Blood 2012;119:2829–2836. doi: 10.1182/blood-2011-11-390807
4. Franzoi AC, Araujo AQ. Disability and determinants of gait performance in tropical spastic paraparesis/HTLV-I associated myelopathy (HAM/TSP). Spinal Cord 2007;45:64–68.
5. Yamano Y, Sato T. Clinical pathophysiology of human T-lymphotropic virus-type 1-associated myelopathy/tropical spastic paraparesis. Front Microbiol 2012;3:389. doi: 10.3389/fmicb.2012.00389
6. Kannagi M, Harashima N, Kurihara K, et al. Tumor immunity against adult T-cell leukemia. Cancer Sci 2005;96:249–255.
7. Shublaq M, Orsini M, Puccioni-Sohler M. Implications of HAM/TSP functional incapacity in the quality of life. Arq Neuropsiquiatr 2011;69(2A):208–211.
8. Semmes OJ, Cazares LH, Ward MD, et al. Discrete serum protein signatures discriminate between human retrovirus-associated hematologic and neurologic disease. Leukemia 2005;19:1229–1238.
9. Kirk PD, Witkover A, Courtney A, et al. Plasma proteome analysis in HTLV-1-associated myelopathy/tropical spastic paraparesis. Retrovirology 2011;8:81. doi: 10.1186/742-4690-8-81
10. Rahman S, Quann K, Pandya D, et al. HTLV-1 Tax mediated downregulation of miRNAs associated with chromatin remodeling factors in T cells with stably integrated viral promoter. PLoS One 2012;7:e34490. doi: 10.1371/journal.pone.0034490
11. Pepe MS, Cai T, Longton G. Combining predictors for classification using the area under the receiver operating characteristic curve. Biometrics 2006;62:221–229.
12. Taylor GP, Goon P, Furukawa Y, et al. Zidovudine plus lamivudine in human T-lymphotropic virus type-I-associated myelopathy: a randomised trial. Retrovirology 2006;3:63.
13. Vincent AJ, Lau PW, Roskams AJ. SPARC is expressed by macroglia and microglia in the developing and mature nervous system. Dev Dyn 2008;237:1449–1462.
14. Lloyd-Burton SM, York EM, Anwar MA, et al. SPARC regulates microgliosis and functional recovery following cortical ischemia. J Neurosci 2013;33:4468–4481.
15. Fredrikson S, Link H, Eneroth P. CSF neopterin as marker of disease activity in multiple sclerosis. Acta Neurol Scand 1987;75:352–355.
16. Karlsen NR, Froland SS, Reinvang I. HIV-related neuropsychological impairment and immunodeficiency. CD8+ lymphocytes and neopterin are related to HIV-encephalopathy. Scand J Psychol 1994;35:230–239.
17. Gasse T, Murr C, Meyersbach P, et al. Neopterin production and tryptophan degradation in acute Lyme neuroborreliosis versus late Lyme encephalopathy. Eur J Clin Chem Clin Biochem 1994;32:685–689.
18. Devaraj S, Glaser N, Griffen S, et al. Increased monocytic activity and biomarkers of inflammation in patients with type 1 diabetes. Diabetes 2006;55:774–779.
19. Izumo S. Neuropathology of HTLV-1-associated myelopathy (HAM/TSP). Neuropathology 2010;30:480–485.

Supporting Information

Additional Supporting Information may be found in the online version of this article:

Table S1. Osame's Motor Disability Score (OMDS).
Table S2. List of peptides with the lowest 100 *P*-values.
Table S3. Prediction of HAM/TSP onset and point of therapeutic intervention with existing markers.
Figure S1. Data acquired in LC/MS/MS analyses were loaded on Refiner MS and 2D-planes represented by mass-to-charge ratio and retention time were generated. To eliminate peaks originated from chemical noises on 2D-planes, four-step Noise Subtraction was conducted. All samples were aligned by retention times and 2D-planes

were merged into a single plane to determine peptide-derived peaks in Summed Peak Detection algorithm. Quantitative information accompanying each peptide was extracted after isotope clustering and statistical analyses were performed.

Figure S2. The classifiers for HAM/TSP onset established with two factors, SPARC and VCAM1 were appraised by area under the curve of ROC curve. Red lines indicate the ROC curves of (A) two factors, (B) SPARC, and (C) VCAM1. Black broken lines show ROC curve of viral load.

Figure S3. The classifiers which distinguished HAM 4–11 from the others were evaluated by AUC. Red lines indicate ROC curves of (A) two factors, (B) SPARC, and (C) VCAM1. Black broken lines indicate viral load.

Clinical & Experimental Neuroimmunology

Clinical and Experimental Neuroimmunology **5** (2014) 108–109

NEW DEVELOPMENT FROM ASIA

Positive feedback loop through astrocytes causes chronic inflammation in human T-lymphotropic virus type 1-associated myelopathy/tropical spastic paraparesis

Human T-lymphotropic virus type 1 (HTLV-1) is a retrovirus infecting 10–20 million people worldwide, 2–3% of whom develop the chronic spinal cord inflammation that characterizes HTLV-1-associated myelopathy/tropical spastic paraparesis (HAM/TSP).[1] Evidence suggests that HTLV-1-infected CD4+ T cells migrate across the blood–brain barrier (BBB) and secrete pro-inflammatory cytokines, such as interferon-gamma (IFN-γ), within the central nervous system.[2] The present authors and others have previously shown that the chemokine CXC motif ligand 10 (CXCL10), which binds the CD4+ T helper type 1 (Th1) receptor CXC motif receptor 3 (CXCR3), stands out as particularly elevated in the cerebrospinal fluid (CSF) of HAM/TSP patients and is well-correlated with disease progression.[3] We therefore hypothesized that chemokines, namely CXCL10, play an important role in the pathogenesis of HAM/TSP by continuously recruiting pro-inflammatory cells to the CNS.

We first confirmed that the CSF of HAM/TSP patients contains extraordinarily high levels of CXCL10 and CXCR3+ cells.[4] Importantly, the levels of CXCL10 were much higher in the CSF than the

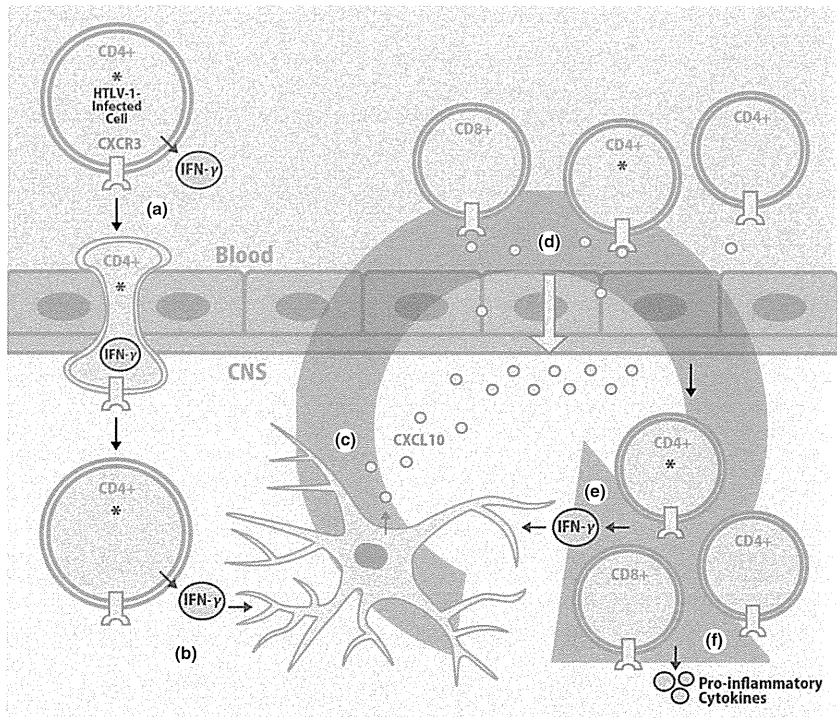

Figure 1 Human T-lymphotropic virus type 1 (HTLV-1)-associated myelopathy/tropical spastic paraparesis (HAM/TSP) pathogenesis comprises an inflammatory positive feedback loop. (a) HTLV-1-infected interferon-gamma (IFN-γ)-producing CD4+ Th1 cells migrate across the blood–brain barrier into the central nervous system, where (b) they produce IFN-γ, (c) which stimulates astrocytes to produce CXCL10. (d) The abundant CXCL10 in the central nervous system (CNS) creates a concentration gradient by which CXCR3-expressing CD4+ and CD8+ T cells undergo chemotaxis to the CNS. (e) These Th1 cells attracted by the CXCL10 also produce pro-inflammatory cytokines including IFN-γ, which further stimulates the astrocytes, (f) creating a positive feedback loop that generates abundant pro-inflammatory cytokines in the CNS. The inflammation in the CNS gradually damages the spinal cord.

serum, yielding a concentration gradient towards the CNS. Additionally, levels of CXCL10 were correlated with known features of HAM/TSP, namely increased CSF cell count. Other chemokines, such as CXCL9, CCL5 and CCL4, were considered but did not show similar trends. We then analyzed samples of peripheral blood mononuclear cells (PBMC), CSF cells, and spinal cord tissue to show that CD4+CXCR3+ cells are indeed infected with HTLV-1, do migrate across the BBB into the CNS and do produce IFN-γ in HAM/TSP patients.

Together, these results show that the pathogenesis of HAM/TSP involves CXCR3+ cells crossing the BBB, at least in part as a result of chemotactic attraction to the abundant CXCL10 in the CNS, and secreting pro-inflammatory cytokines that cause spinal cord inflammation. The question remains: from where does this abundant CXCL10 originate?

Immunohistochemical analysis of the spinal cord tissue not only confirmed that CXCL10 is produced in the spinal cords of HAM/TSP patients, but also showed that astrocytes might be the main producers. Co-culture of human astrocytoma cells with CD4+ T cells from HAM/TSP patients confirmed that astrocytes produce CXCL10 in response to IFN-γ secreted by CD4+ T cells.

We concluded that these astrocytes likely represent the missing piece of the puzzle, and we postulated the existence of an inflammatory positive feedback loop: infected CD4+ T cells cross the BBB and produce IFN-γ, which stimulates astrocytes to produce CXCL10, which recruits more CXCR3+ cells of both CD4+ and CD8+ subtypes to the CNS, where they produce more IFN-γ (Fig. 1). As for the initial trigger that starts the vicious cycle, it is thought that HTLV-1-infected cells could be inherently likely to cross the BBB as a result of HTLV-1-induced expression of certain cell surface proteins.[5]

Finally, chemotaxis assays showed that it might be possible to disrupt this loop with anti-CXCL10 neutralizing antibodies. As the current data points to a virtually exclusively Th1-dominant pathogenesis, disruption of the Th1 inflammatory process could effectively cure the disease.

Thus, we described a Th1-centric inflammatory positive feedback loop critical for HAM/TSP pathogenesis and suggested that disrupting this loop might lead to a cure.

References

1. Osame M, Usuku K, Izumo S, et al. HTLV-I associated myelopathy, a new clinical entity. *Lancet*. 1986; **1**: 1031–2.
2. Yamano Y, Sato T. Clinical pathophysiology of human T-lymphotropic virus-type 1-associated myelopathy/tropical spastic paraparesis. *Front Microbiol*. 2012; **3**: 389.
3. Sato T, Coler-reilly A, Utsunomiya A, et al. CSF CXCL10, CXCL9, and neopterin as candidate prognostic biomarkers for HTLV-1-associated myelopathy/tropical spastic paraparesis. *PLoS Negl Trop Dis*. 2013; **7**(10): e2479.
4. Ando H, Sato T, Tomaru U, et al. Positive feedback loop via astrocytes causes chronic inflammation in virus-associated myelopathy. *Brain*. 2013; **136**(Pt 9): 2876–87.
5. Yamamoto-Taguchi N, Satou Y, Miyazato P, et al. HTLV-1 bZIP factor induces inflammation through labile Foxp3 expression. *PLoS Pathog*. 2013; **9**: e1003630.

Ariella Coler-Reilly, Hitoshi Ando and Yoshihisa Yamano

Department of Rare Diseases Research, Institute of Medical Science, St. Marianna University School of Medicine, Kanagawa, Japan

SpringerPlus
a SpringerOpen Journal

CASE STUDY Open Access

A case of post-transplant adult T-cell leukemia/lymphoma presenting myelopathy similar to but distinct from human T-cell leukemia virus type I (HTLV- I)-associated myelopathy

Toyotaka Kawamata[1*], Nobuhiro Ohno[1], Kota Sato[1,2], Masayuki Kobayashi[1,2], Norihide Jo[1], Koichiro Yuji[1], Ryuji Tanosaki[3], Yoshihisa Yamano[4], Arinobu Tojo[1,2] and Kaoru Uchimaru[1]

Abstract

Introduction: Adult T-cell leukemia/lymphoma (ATL) responds poorly to conventional chemotherapy, but allogeneic stem cell transplantation (allo-SCT) may improve disease prognosis. Herein, we report a female patient with human T-cell leukemia virus type I (HTLV-I)-associated myelopathy (HAM)-like myelopathy following allo-SCT for ATL.

Case report: She developed crural paresis 14 months after allo-SCT. Initially, she was diagnosed with central nervous system (CNS) relapse of ATL and treated with intrathecal injection and whole brain and spine irradiation. Her symptoms recurred 5 months later, when a cerebrospinal fluid (CSF) specimen showed increased CD4 + CXCR3 + CCR4+ cell numbers and levels of neopterin and CXCL10 (IP-10).

Discussion: These results suggest the possible involvement of a certain immunological mechanism such as HAM in her symptoms, irrespective of the lack of anti-HTLV-I antibody in her CSF. Because a definitive diagnosis of CNS manifestation of ATL is sometimes difficult, multi-modal laboratory data are required for differential diagnosis.

Keywords: Adult T-cell leukemia/lymphoma; Post-transplant myelopathy; HTLV-I-associated myelopathy (HAM); Neopterin; CXCL10 (IP-10)

Introduction

Human T-cell leukemia virus type I (HTLV-I) was the first retrovirus identified in humans, isolated from a patient with cutaneous lymphoma (Poiesz et al. 1980). HTLV-I is the cause of not only adult T-cell leukemia/lymphoma (ATL) (Uchiyama et al. 1977; Hinuma et al. 1981) but also HTLV-I-associated myelopathy (HAM)/tropical spastic paraparesis (TSP) (Osame et al. 1986), HTLV-I-associated uveitis (HU) (Ohba et al. 1989; Mochizuki et al. 1992) and infective dermatitis (McGill et al. 2012; de Oliveira et al. 2010).

ATL is one of the most intractable T-cell malignancies, and it responds poorly to conventional chemotherapy, with a median survival time (MST) of approximately 8 months (Shimoyama et al. 1988). Among such treatments, modified LSG-15 (mLSG-15) has shown the best results; in a previous study, the progression free survival (PFS) at 1 year among patients treated with mLSG-15 was 28% and the overall survival (OS) at 3 years was 24% (Tsukasaki et al. 2007). However, the improvement in survival time by mLSG-15 treatment is not satisfactory. Allo-HSCT is a promising treatment option to cure ATL because it may improve disease prognosis (Utsunomiya et al. 2001; Kami et al. 2003).

Herein, we describe a case of HAM-like myelopathy that was difficult to distinguish from central nervous system (CNS) relapse of ATL following allogeneic peripheral blood stem cell transplantation. This case report suggests that there might be immunological myelopathy after HSCT. In the present case, flow cytometric analysis of the cells in cerebrospinal fluid (CSF) was helpful to differentiate it from CNS relapse of ATL.

* Correspondence: toyotaka@ims.u-tokyo.ac.jp
[1]Department of Hematology/Oncology, Research Hospital, The Institute of Medical Science, the University of Tokyo, 4-6-1 Shirokanedai, Minato-ku, Tokyo 108-8639, Japan
Full list of author information is available at the end of the article

Case report

A 63-year-old female patient recognized cervical lymph nodes swelling in October 2010. Lactate dehydrogenase (LDH) and serum corrected calcium levels kept within normal limit, but soluble interleukin-2 receptor (sIL-2R) elevated significantly at the initial visit (Table 1). Diagnostic imaging by computed tomography (CT) revealed systemic lymphadenopathies (cervical, axial, mediastinal, abdominal and mesenteric lymphadenopathy) before the following chemotherapy. Although appetite loss and abdominal distention were added with lymphadenopathy, any other abnormal finding of physical examination could not be detected. Her ECOG performance status was grade 1 before chemotherapy. She received cervical lymph node biopsy and pathological findings of cervical lymph node revealed T cell lymphoma compatible, and HTLV-I provirus DNA analysis (Southern blot) revealed monoclonal integration. Abnormal lymphocytes were not detected in peripheral blood (PB) and HTLV-I provirus DNA analysis of PB did not show monoclonal integration. She was diagnosed as ATL (lymphoma type). She has past histories of glaucoma and pulmonary cryptococcosis. None of ATL patient was in her family.

She was referred to our hospital and received four sessions of mLSG-15 therapy in our hospital. Prophylactic intrathecal injection was performed twice, during chemotherapy and before allogeneic stem cell transplantation. No meningeal involvement of ATL cells was detected at that time. She went into complete remission (Response criteria for adult T cell leukemia-lymphoma from an international consensus meeting (Tsukasaki et al. 2009)) in April 2011. She received following allogeneic peripheral blood stem cell transplantation (allo-PBSCT) in the National Cancer Center Hospital (Tokyo, Japan) (Figure 1). The transplantation conditioning regimen consisted of fludarabine (30 mg/m^2 per day for 5 days) plus busulfan (3.2 mg/kg per day for 2 days) and only cyclosporine A (CyA) was used for GVHD prophylaxis. Transplanted CD34-positive cells were 2.67×10^6/kg and rapid engraftment was achieved. Grade III (gastrointestinal tract and skin) acute graft-versus-host disease (GVHD) was observed 1 month after transplantation, but it improved after treatment with methylpredonisolone (mPSL) (1 mg/kg). No chronic GVHD was observed. CyA was tapered gradually and discontinued 9 months after transplantation, in February 2012. After that point, only 5 mg/day predonisolone (PSL) was continued.

In July 2012 (14 months after allo-PBSCT), the patient developed hemiparesis of the left side. Although left upper-limb paresis improved, lower-extremity paresis progressed to paraplegia. Magnetic resonance imaging (MRI) revealed multiple high-intensity lesions in T2-weighted images of the medulla oblongata, cervical spinal cord, and thoracic spinal cord (Figure 2A), and a CSF specimen showed increased cell counts (Figure 3). Morphologically, typical ATL cells such as flower cells were not detected in CSF, but abnormal small to middle size lymphocytes indistinguishable from ATL cells increased. She was diagnosed as CNS relapse of ATL, and received mPSL pulse, intrathecal injection of MTX 15 mg + Ara-C 40 mg + PSL 20 mg, and irradiation of the whole brain and spine. Following these treatments, the paraplegia improved gradually to such a degree that she could walk with a walker. During the course of these treatments, she was complicated by neurogenic bladder dysfunction, and diabetes insipidus.

In January 2013 (20 months after allo-PBSCT), she again developed left lower-limb weakness, which gradually progressed. She was admitted to our hospital in February 2013. On admission, neurological examination revealed

Table 1 Laboratory data of onset of ATL (lymphoma type) in October 2010

WBC	4100/μl	GOT	67 IU/L	CRP	0.06 mg/dl
Myelo	1.0%	GPT	72 IU/L	sIL-2R	5802 U/ml
St	8.0%	LDH	215 IU/L		
Seg	71.0%	ALP	277 IU/L	HTVL-I Ab	(+)
Ly	11.0%	γ-GTP	46 IU/L	HBs-Ag	(–)
Mo	8.0%	Alb	3.5 mg/dl	HBs-Ab	(–)
Baso	1.0%	BUN	15.6 mg/dl	HBc-Ab	(–)
RBC	423×10^4/μl	Cre	0.58 mg/dl	HCV-Ab	(–)
Hb	13.2 g/dl	Na	142.4 mEq/L	HIV-Ab	(–)
Hct	39.0%	K	4.2 mEq/L	TPHA	(–)
MCV	92.2 fl	Cl	103.8 mEq/L		
MCH	31.2 pg	Corrected Ca	9.9 mg/dl		
MCHC	33.8%				
Plt	21.9×10^4/μl				

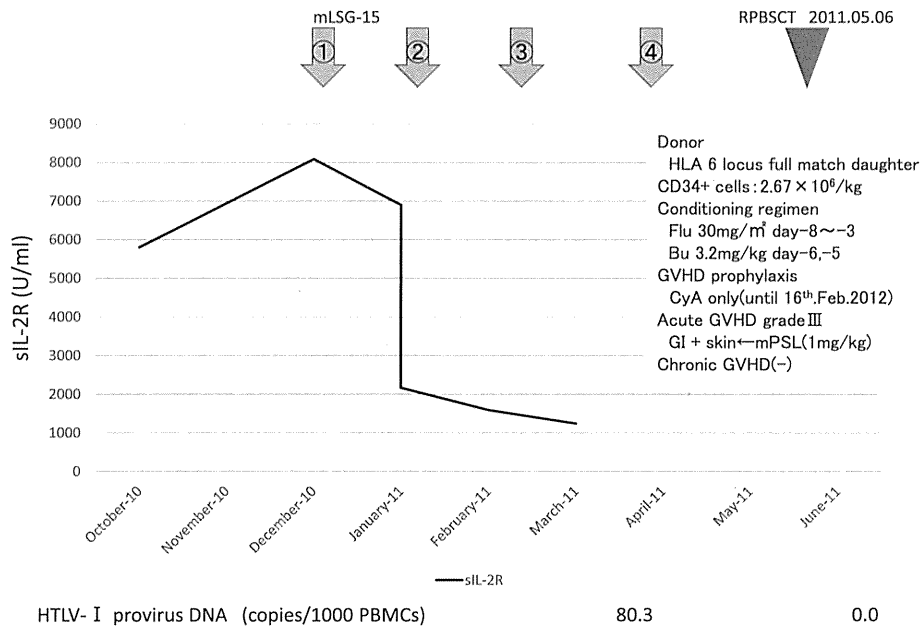

Figure 1 Clinical course from conventional chemotherapy (mLSG-15) to allogeneic peripheral blood stem cell transplantation. The patient received four sessions of mLSG-15 therapy and achieved complete remission (CR) before receiving allo-PBSCT.

no abnormality of cranial nervous system, but abnormal reflex such as Babinski and Chaddock reflex in bilateral lower-limb. Thermal hypoalgesia under right Th4 and left Th6 dermatome was detected, but tactile sense was intact. She was accompanied with bladder dysfunction and severe constipation. Brain and spinal MRI revealed a residual spinal lesion at Th3-7 (Figure 2B). The cell numbers in CSF did not increase, but myelin basic protein (MBP) level was elevated (Figure 4B). Morphologically, ATL cells could not be detected in CSF. Flow cytometric analysis to determine the specific immunophenotype of CD4+ lymphocytes in CSF revealed an expansion of the $CD4^+CXCR3^+CCR4^+$

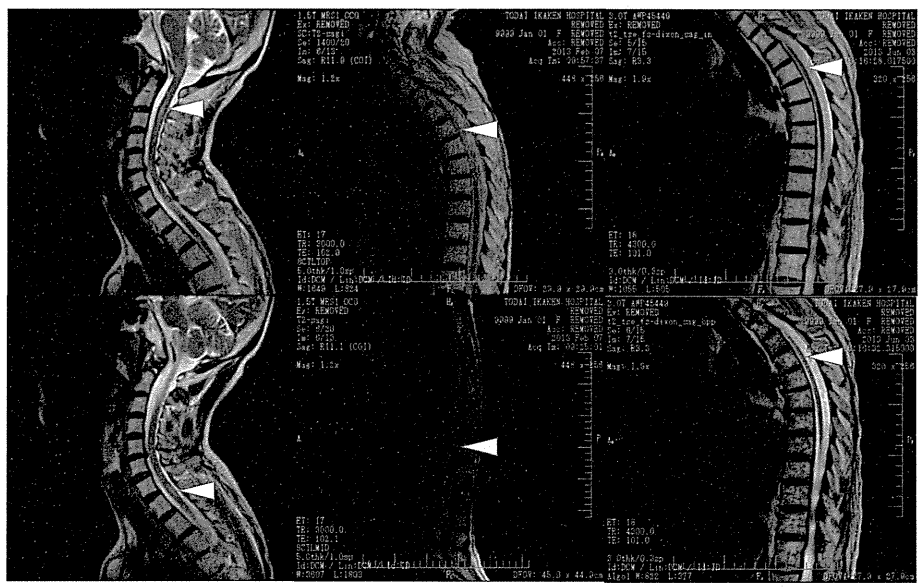

Figure 2 MRI findings. A) At the onset of neurogenic disorder in July 2012. Multiple high-intensity lesions in T2-weighted images (T2WI) of the medulla oblongata, cervical spinal cord, and thoracic spinal cord were revealed. **B)** Residual high-intensity lesion in Th3-7. **C)** Following treatment, the residual lesion in the thoracic spinal cord improved.

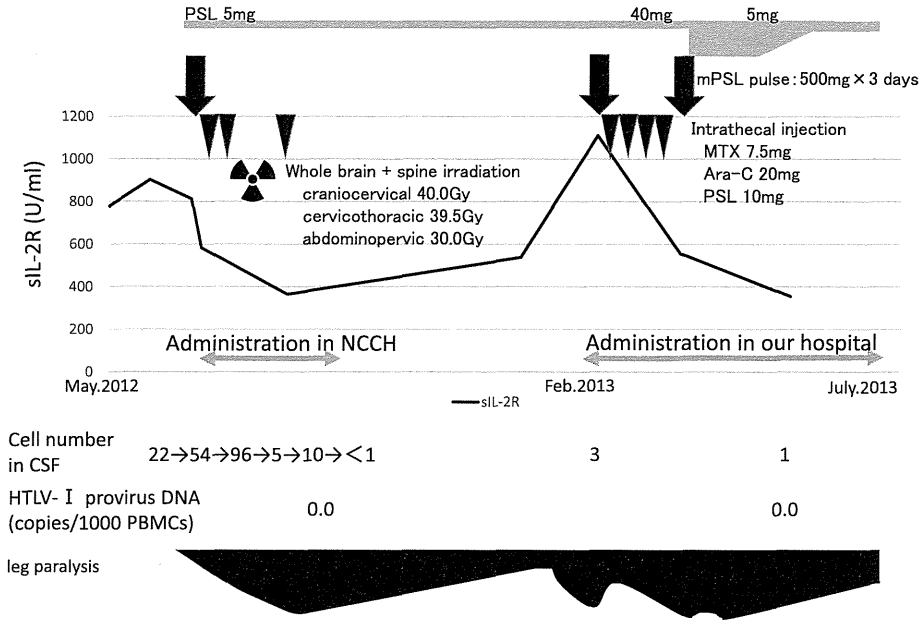

Figure 3 Clinical course after onset of the neurogenic disorder. The patient developed paraplegia 14 months after allo-PBSCT. Neurological findings were partially relieved following treatment with a high dose of mPSL accompanied by intrathecal injection of MTX + Ara-C + PSL and irradiation of the whole brain and spine. Three months later, her neurological deficit worsened again. Ultimately, her neurological disorder improved after treatment with a high dose of steroid.

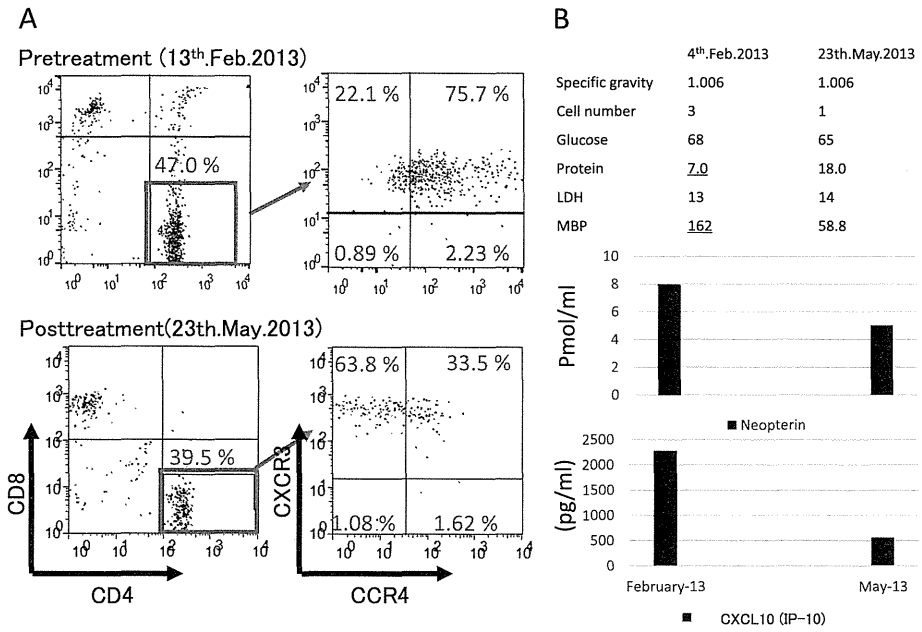

Figure 4 CSF findings. A) Flow cytometric analysis of CSF. Before treatment, the CD4 + CXCR3 + CCR4+ cell population was predominantly elevated. Following treatment, it decreased and the CD4 + CXCR3 + CCR4- cell population increased. **B)** Neopterin and CXCL10 (IP-10) concentrations in CSF. Before treatment, both neopterin and CXCL10 (IP-10) concentrations were significantly elevated. Following treatment, both biomarkers decreased to within the range of the therapeutic goal for HAM patients.

cell population (Figure 4A), which conflicted with CNS relapse of ATL but was consistent with HAM (Natsumi et al. 2014). Furthermore, both the neopterin and CXCL10 (IP-10) concentrations in the CSF were significantly elevated (Figure 4B), although lower than those associated with aggressive HAM (14). Notably, the case was insufficient to fulfill the diagnostic criteria for HAM (Mitsuhiro 1990) because HTLV-I antibody (PA method) was negative in CSF.

Bacterial, fungal, and tuberculous encephalomyelopathies were excluded because no increase in cell numbers and no decline in glucose concentration in CSF were observed. Real-time polymerase chain reaction (PCR) testing for CMV, EBV, HSV, VZV, HHV-6, and JC virus in CSF showed negative results.

Serum soluble interleukin-2 receptor (sIL-2R) level was slightly elevated (Table 2), but significantly lower compared with that at the onset of ATL.

Not all of the results necessarily corresponded to CNS relapse of ATL, although we could not exclude it. We treated her with mPSL pulse and intrathecal injection of MTX + Ara-C + PSL. After one course of mPSL pulse, her crural paresis improved dramatically to such a degree that she could pull up to standing after a few days. Although she was given intrathecal injections four times weekly, her crural paresis was gradually exacerbated and progressed to paralysis. mPSL pulse was performed again, but the effect was limited.

We examined her CSF again but there was no increase in cells, and ATL cells could not be detected by microscopic examination. Furthermore, the MRI findings improved over time (Figure 2C), although her neurological findings worsened and HTLV-I proviral DNA could not be detected repeatedly in peripheral mononuclear cells (PBMCs) after allo-PBSCT. No evidence of relapsed ATL could be found and we continued 5 mg/day PSL thereafter while she continued rehabilitation.

The results of CSF analysis in May 2013 showed the following improvements. In flow cytometric analysis, the CD4 + CXCR3 + CCR4+ cell population had decreased and the normal CD4 + CXCR3 + CCR4- cell population had increased. Both neopterin and CXCL10 (IP-10) had decreased to within the range of the therapeutic goal for HAM patients (Figure 4A,B). Her paralysis improved gradually and steadily only by rehabilitation, to such a degree that she could walk when holding onto parallel bars.

Discussion

ATL with CNS involvement may occur during systemic progression of the disease and its frequency is estimated to be 10–25% (Kitajima et al. 2002). However, cases of CNS relapse without peripheral blood and lymph nodes of ATL have been reported (Marshall et al. 1998; Dungerwalla et al. 2005). In flow cytometric analysis of CSF of ATL patients, the CD4 + CXCR3-CCR4+ cell population is elevated. However, in the current case, the CSF fluid analysis revealed expansion of the CD4 + CXCR3 + CCR4+ cell population, which is consistent with HAM (Natsumi et al. 2014). Sato T et al. (Sato et al. 2013) reported increased neopterin and CXCL10 (IP-10) in HAM patients, and they were valuable biomarkers for disease progression of HAM. The neopterin and CXCL10 (IP-10) concentration in CSF paralleled the disease activity of HAM. The cut-off concentrations of neopterin and CXCL10 in HAM/TSP patients compared to HTLV-I infected non-HAM subjects are less than 5 pmol/mL and 200 pg/ml, respectively, and the CXCL10 (IP-10) concentration in the CSF of HAM patients with rapid progression is usually more than 5,000 pg/mL (Yamono, Y., personal communication). In the current case, we could not make a diagnosis of HAM because the CSF was negative for HTLV-I antibody in repeated examinations. Although the immunosuppressive status after allo-PBSCT might contribute, serum immunoglobulin levels

Table 2 Laboratory data on admission to our hospital in January 2013

WBC	4470/μl	GOT	15 IU/L	CRP	0.24 mg/dl
St	1.5%	GPT	33 IU/L	IgG	1390 mg/dl
Seg	64.0%	LDH	199 IU/L	IgA	51 mg/dl
Ly	14.0%	ALP	453 IU/L	IgM	352 mg/dl
Mo	19.5%	γ-GTP	87 IU/L		
Abnormal Ly	1.0%	TP	6.7 mg/dl	HTVL-I Ab	(+)
RBC	302×10^4/μl	Alb	3.5 mg/dl	HBs-Ag	(–)
Hb	9.5 g/dl	BUN	9.8 mg/dl	HBs-Ab	(–)
Hct	29.4%	Cre	0.56 mg/dl	HBc-Ab	(–)
MCV	97.4 fl	Na	133 mEq/L	HCV-Ab	(–)
MCH	31.5 pg	K	4.0 mEq/L	HIV-Ab	(–)
MCHC	32.3%	Cl	96 mEq/L		
Plt	12.0×10^4/μl	Corrected Ca	10.5 mg/dl		

were almost within normal limit at the same time period (Table 2) and there is not enough evidence to indicate false negative. In any inflammatory diseases of CNS, CXCR3+ cells but not CCR4+ cells were generally found in CSF (Misu et al. 2001). However, CXCR3 + CCR4+ double positive cells existed in her CSF. It was unlikely that CXCR3 + CCR4+ double positive cells emerged into CSF in nonspecific inflammatory condition. Given her background, we supposed these CCR4+ cells were HTLV-I infected cells, but the number of these cells was insufficient to measure HTLV-I viral load.

In the current case, neither CSF data nor clinical course consisted with CNS relapse of ATL. In case of ATL patients, CXCR3-CCR4+ T cell lymphocytes population expanded. Therapeutic effect was obtained from mPSL pulse rather than intrathecal injection. Furthermore, disease progression in the typical case of CNS relapse of ATL was more aggressive. We concluded some inflammatory condition caused by these HTLV-I infected cells may have developed HAM-like myelopathy.

CNS GVHD remains a controversial entity and it is difficult to establish an unequivocal diagnosis. Yet a few cases have been reported, who were suspected of CNS GVHD from brain biopsy or autopsy, their CSF showed predominant T-lymphocyte infiltration of donor origin (Kamble et al. 2007). In the current case, brain or spinal cord biopsy was not performed, and chimerism analysis of T cells in CSF was difficult because of the full-match HLA and sex-matched PBSCT. The number of T cells in CSF was insufficient to analyze chimerism using the short tandem repeat (STR) method. Neopterin (Niederwieser et al. 1984; Hempel et al. 1997) and CXCL10 (IP-10) (Mapara et al. 2006) levels in serum increase significantly in patients with active GHVD, but the levels in CSF are unknown. The possibility of active CNS GVHD could not be completely excluded. Both CXCR3 and CCR4 expression of T cells infiltrated in the CNS in patients with active CNS GVHD is unknown. It was no wander that CXCR3+ cells in CSF were found in nonspecific inflammatory condition such as CNS GVHD, but unlikely that CCR4+ cells were.

The patient's neurological dysfunction seemed to fluctuate in parallel with the serum concentration of soluble interleukin-2 (sIL-2R) receptor (Figure 3). However, increased sIL-2R occurs not only with ATL relapse but also with HAM (Matsumoto et al. 1990), GVHD (Kami et al. 2000), and inflammatory neurogenic disorders caused by immunologic T-cell responses (Maier et al. 2009). Thus, it is difficult to make a definite diagnosis based on elevated sIL-2R alone.

In conclusion, we report a case with myelopathy without ATL relapse in the CNS. Flow cytometric analysis is helpful to differentiate immune-mediated encephalopathy or myelopathy from CNS relapse of ATL. If we encountered the patients suspected of CNS relapse of ATL, we should consider the possibility of inflammatory condition caused by HTLV-I infected cells. Further analysis of pathology are warranted.

Competing interests
The authors declare that they have no competing interests.

Authors' contribution
TK participated in treatment for the patient and drafting the manuscript. NO, KS, MK, NJ and KY participated in treatment for the patient. YY carried out flow cytometric analysis and measurement of neopterin and CXCL10 (IP-10) concentration in CSF, and helped to draft the manuscript. RT participated in acquiring the data and helping to draft the manuscript. AT and KU supervised and helped to draft the manuscript. All authors read and approved the final manuscript.

Author details
[1]Department of Hematology/Oncology, Research Hospital, The Institute of Medical Science, the University of Tokyo, 4-6-1 Shirokanedai, Minato-ku, Tokyo 108-8639, Japan. [2]Division of Molecular Therapy, Department of The advanced Clinical Research Center, The Institute of Medical Science, the University of Tokyo, 4-6-1 Shirokanedai, Minato-ku, Tokyo 108-8639, Japan. [3]Department of Blood Transfusion and Cellular Therapy, National Cancer Center Hospital, 5-1-1 Tsukiji, Chuo-ku, Tokyo 104-0045, Japan. [4]Department of Rare Diseases Research, Institute of Medical Science, St. Marianna University Graduate School of Medicine, Sugao, Miyamae-ku, Kawasaki, Kanagawa 216-8512, Japan.

Received: 15 August 2014 Accepted: 22 September 2014
Published: 4 October 2014

References
de Oliveira MF, Vieira M, Primo J, Siqueira IC, Carvalho EM, Farre L, Fatal PL, Bittencourt AL (2010) Flower cells in patients with infective dermatitis associated with HTLV-1. J Clin Virol 48:288–290

Dungerwalla M, Osuji N, Waldman AD, Jehani FAI, Mehta A, Taylor R, Wotherspoon A, Cogill G, Matutes E (2005) Isolated central nervous system involvement in adult T-cell lymphoma/leukaemia. Br J Haematol 130:511–515

Hempel L, Körholz D, Nussbaum P, Bönig H, Burdach S, Zintl F (1997) High interleukin-10 serum levels are associated with fatal outcome in patients after bone marrow transplantation. Bone Marrow Transplant 20:365–368

Hinuma Y, Nagata K, Hanaoka M, Nakai M, Matsumoto T, Kinoshita K, Shirakawa S, Miyoshi I (1981) Adult T-cell leukemia: antigen in an ATL cell line and detection of antibodies to the antigen in human sera. Proc Natl Acad Sci U S A 78:6476–6480

Kamble RT, Chang CC, Sanchez S, Carrum G (2007) Central nervous system graft-versus-host disease: report of two cases and literature review. Bone Marrow Transplant 39:49–52

Kami M, Matsumura T, Tanaka Y, Mikami Y, Miyakoshi S, Ueyama J, Morinaga S, Mori S, Machida U, Kanda Y, Chiba S, Sakamaki H, Hirai H, Muto Y (2000) Serum levels of soluble interleukin-2 receptor after bone marrow transplantation: a true marker of acute graft-versus-host disease. Leuk Lymphoma 38:533–540

Kami M, Hamaki T, Miyakoshi S, Murashige N, Kanda Y, Tanosaki R, Takaue Y, Tanigushi S, Hirai H, Ozawa K, Kasai M (2003) Allogeneic haematopoietic stem cell transplantation for the treatment of adult T-cell leukaemia/lymphoma. Br J Haematol 120:304–309

Kitajima M, Korogi Y, Shigematsu Y, Murashige M, Kanda Y, Tanosaki R, Takaue Y, Taniguchi S, Hirai H, Ozawa K, Kasai M (2002) Central nervous system lesions in adult T-cell leukaemia: MRI and pathology. Neuroradiology 44:559–567

Maier LM, Anderson DE, Severson CA, Baecher-Allan C, Healy B, Liu DV, Wittrup KD, De Jager PL, Hafler D (2009) Soluble IL-2RA levels in multiple sclerosis subjects and the effect of soluble IL-2RA on immune responses. J Immunol 182:1541–1547

Mapara MY, Leng C, Kim YM, Bronson R, Loksbin A, Luster A, Sykes M (2006) Expression of chemokines in GVHD target organs is influenced by conditioning and genetic factors and amplified by GVHR. Biol Blood Marrow Transplant 12:623–634

Marshall AG, Pawson R, Thom M, Shuz TF, Scaravilli F, Rudge P (1998) HTLV-I associated primary CNS T-cell lymphoma. J Neurol Sci 158:226–231

Matsumoto M, Sugimoto M, Nakashima H, Imamura F, Kawano O, Uyama E, Takatsu K, Araki S (1990) Spontaneous T cell proliferation and release of

soluble interleukin-2 receptors in patients with HTLV-I-associated myelopathy. Am J Trop Med Hyg 42:365–373

McGill NK, Vyas J, Shimauchi T, Tokura Y, Piguet V (2012) HTLV-1-associated infective dermatitis: updates on the pathogenesis. Exp Dermatol 21:815–821

Misu T, Onodera H, Fujihara K, Matsushima K, Yoshie O, Okita N, Takase S, Itoyama Y (2001) Chemokine receptor expression on T cells in blood and cerebrospinal fluid at relapse and remission of multiple sclerosis: imbalance of Th1/Th2-associated chemokine signaling. J Neuroimmunol 114:207–212

Mitsuhiro O (1990) Review of WHO kagoshima meeting and diagnostic guidelines for HAM/TSP. Raven Press, New York, pp 191–197

Mochizuki M, Watanabe T, Yamaguchi K, Yoshimura K, Nakashima S, Shirao M, Araki S, Takatsuki K, Mori S, Miyata N (1992) Uveitis associated with human T-cell lymphotropic virus type I. Am J Ophthalmol 114:123–129

Natsumi A, Tomoo S, Hitoshi A, Yoshihisa Y (2014) HTLV-1 induces a Th1-like state in CD4+CCR4+ T cells. J Clin Invest 124:3431–3442

Niederwieser D, Huber C, Gratwohl A, Bannert P, Fuchs D, Hausen A, Reibnegger D, Speck B, Wachter H (1984) Neopterin as a new biochemical marker in the clinical monitoring of bone marrow transplant recipients. Transplantation 38:497–500

Ohba N, Matsumoto M, Sameshima M, Kabayama Y, Nakao K, Unoki K, Uehara F, Kawano K, Maruyama I, Osame M (1989) Ocular manifestations in patients infected with human T-lymphotropic virus type I. Jpn J Ophthalmol 33:1–12

Osame M, Usuku K, Izumo S, Ijichi N, Amitani H, Igata A, Matsumoto M, Tara M (1986) HTLV-I associated myelopathy, a new clinical entity. Lancet 1:1031–1032

Poiesz BJ, Ruscetti FW, Gazdar AF, Bunn PA, Minna JD, Gallo RC (1980) Detection and isolation of type C retrovirus particles from fresh and cultured lymphocytes of a patient with cutaneous T-cell lymphoma. Proc Natl Acad Sci U S A 77:7415–7419

Sato T, Coler-Reilly A, Utsunomiya A, Araya N, Yagishita N, Ando H, Yamauchi J, Inoue E, Ueno T, Hasegawa Y, Nishioka K, Nagajima T, Jacobson S, Izumo S, Yamano Y (2013) CSF CXCL10, CXCL9, and neopterin as candidate prognostic biomarkers for HTLV-1-associated myelopathy/tropical spastic paraparesis. PLoS Negl Trop Dis 7:e2479

Shimoyama M, Ota K, Kikuchi M, Yunoki K, Konda S, Takatsuki K, Ichimaru M, Tominaga S, Tsugane S, Minato K, Tobinai K, Oyama A, Hisano S, Matsumoto M, Takiguchi T, Yamaguchi K, Kinoshita K, Tajima K, Suemasu K (1988) Major prognostic factors of adult patients with advanced T-cell lymphoma/leukemia. J Clin Oncol 6:1088–1097

Tsukasaki K, Utsunomiya A, Fukuda H, Shibata T, Fukushima T, Takatsuka Y, Ikeda S, Masuda M, Nagoshi H, Ueda R, Tamura K, Sano M, Momita S, Yamaguchi K, Kawano F, Hanada S, Tobinai K, Shimoyama M, Hotta T, Tomonaga M (2007) VCAP-AMP-VECP compared with biweekly CHOP for adult T-cell leukemia-lymphoma: Japan Clinical Oncology Group Study JCOG9801. J Clin Oncol 25:5458–5464

Tsukasaki K, Hermine O, Bazarbachi A, Ratner L, Ramos JC, Harrington W, Jr, O'Mahony D, Janik JE, Bittencourt AL, Taylor GP, Yamaguchi K, Utsunomiya A, Tobinai K, Watanabe T (2009) Definition, prognostic factors, treatment, and response criteria of adult T-cell leukemia-lymphoma: a proposal from an international consensus meeting. J Clin Oncol 27:453–459

Uchiyama T, Yodoi J, Sagawa K, Takatsuki K, Uchino H (1977) Adult T-cell leukemia: clinical and hematologic features of 16 cases. Blood 50:481–492

Utsunomiya A, Miyazaki Y, Takatsuka Y, Hanada S, Uozumi K, Yashiki S, Tara M, Kawano F, Saburi Y, Kikuchi H, Hara M, Sao H, Morishima Y, Kodera Y, Sonoda S, Tomonaga M (2001) Improved outcome of adult T cell leukemia/lymphoma with allogeneic hematopoietic stem cell transplantation. Bone Marrow Transplant 27:15–20

doi:10.1186/2193-1801-3-581
Cite this article as: Kawamata *et al.*: A case of post-transplant adult T-cell leukemia/lymphoma presenting myelopathy similar to but distinct from human T-cell leukemia virus type I (HTLV- I)-associated myelopathy. *SpringerPlus* 2014 3:581.